

## Complex dielectric spectroscopy of soil using multiple reflection analysis on TDR signal

Yin Jeh Ngui<sup>1</sup> and C.-P. Lin<sup>1</sup>

<sup>1</sup> Department of Civil Engineering, National Chiao Tung University, 1001 Ta-Hsueh Road, Hsinchu, Taiwan.

### ABSTRACT

Soil is a compound material with complex mechanical and electrical properties due to the interactions between soil solids, water, air and occasionally contaminants. Dielectric spectroscopy is capable of revealing the complex behavior and the frequency dependency of its electrical properties. Nevertheless, precise input source, sophisticated calibration and tedious measurement are required in current dielectric spectroscopy measurement techniques. This study adopted the multiple reflection analysis (MRA) approach on time domain reflectometry (TDR) signals to measure the complex dielectric permittivity (CDP) spectrum. MRA is a robust algorithm which extracts CDP spectrum by comparing and inverting the spectral ratios of the first top reflection and the subsequent multiple reflections of TDR signal. This study studied two compacted soil type with various moisture content combinations to investigate the effect of moisture content and dry density to their CDP spectrum. CDP spectrums of the soil-under-test were measured with TDR MRA for frequency range from 10 MHz to 1 GHz. MRA is particularly appropriate for in-situ soil CDP spectroscopy since MRA is source function independent, only requires model-free inversion and simple system parameter calibration. Additional soil types should be studied in order to establish a dielectric spectrum library for further soil parameter investigation.

**Keywords:** TDR, multiple reflection analysis, complex dielectric permittivity, dielectric spectroscopy, soil, moisture content

### 1 INTRODUCTION

Soil medium is a compound material with complex mechanical and electrical properties, consisting of soil solids, water, air and occasionally contaminants. Dielectric spectroscopy of soil is capable of revealing the complex frequency dependency of its electrical properties. This enabled the characterization of the polarization, relaxation and energy dissipation behavior of soil medium at different frequency range. The influence of soil type, moisture content, electrical conductivity and dry density to the dielectric behavior of soil-water mixtures maybe investigated through this powerful tool (Lin 2003). Various volumetric mixing models were developed in order to describe the complex dielectric behavior due to the interactions between the soil particles, bound water, free water and air (Dobson et al. 1985; Heimovaara 1994). These models may represent the actual dielectric dispersion of soils better than conventional Debye equation, which usually describes simpler dielectric characteristic of dynamic polarization with only single relaxation time.

Nonetheless, current complex dielectric permittivity (CDP) spectroscopy is mostly conducted in laboratory due to their tedious acquisitions process, complicated system setup and calibrations, such vector network analyzer (VNA) or frequency domain reflectometry (FDR). Rapid field measurement of soil CDP is still

limited to the single-valued apparent dielectric constant using time domain reflectometry (TDR) for soil moisture measurement. Soil moisture content correlation using apparent dielectric constant is often affected by the risetime of the step pulse, relaxation frequency and the electrical conductivity (EC) (Lin 2003). This may lead to the soil type and density dependency of the soil moisture calibration function. Rich dielectric information of in-situ soil is yet to be gathered and studied for potential correlation in the variation of density and soil structure.

A simple robust phase velocity analysis (PVA) method was recently proposed by Lin et al. (2017) to determine frequency-dependent apparent dielectric constant from the top and end reflections in a TDR signal. This novel approach enabled the rapid measurement of apparent dielectric spectroscopy in field. However, the applicable frequency is much limited by the signal truncation and the real and imaginary parts of dielectric permittivity are not yet decoupled. Lin et al. (2018) later proposed an innovative multiple reflection analysis (MRA) of TDR signals to measure the complete CDP spectrum. The rapid, robust and model-free approach decomposes the TDR signal into the first top reflection ( $r_1$ ) and the remaining multiple reflections ( $r_{remaining}$ ). The spectral ratio of these two parts (MRA ratio) is next theoretically derived as a function of the complex dielectric permittivity, which is independent of source

function (Lin et al. 2018) and as shown below:

$$MRA = \frac{R_{remaining}}{R_1} = \frac{H \cdot (1 - \rho_1^2)}{\rho_1 \cdot (1 + \rho_1 H)} \quad (1)$$

where  $\rho_1$  is the reflection coefficient at interface between probe head and sensing section, while  $H$  is the propagation function of electromagnetic (EM) wave within the sensing probe section defined as below:

$$H = \exp \left[ -\frac{4L\pi f}{c} \sqrt{\varepsilon^*(f)} \right] \quad (2)$$

in which  $L$  is the sensing probe length,  $f$  is the frequency,  $c$  is the speed of light and  $\varepsilon^*(f)$  is the frequency-dependent CDP.

Based on this theoretical formulation, the complex dielectric permittivity can be uniquely inverted from the measured MRA ratio for frequency range of 10 MHz to 1 GHz. Straightforward MRA signal processing algorithm enables dielectric spectroscopy of materials to be conveniently conducted in both laboratory and field, without complicated system setup and calibration. This study followed the detailed signal processing approaches and optimization procedures of MRA, and adopted the iterated initial guess method for CDP inversion according to Lin et al. (2018).

## 2 METHODOLOGY

### 2.1 Experiment setup

Laboratorial measurement setup for measuring the TDR signal of soils is consisted of a broadband TDR reflectometer, a 10m 93  $\Omega$  coaxial cable, a 0.112m 93  $\Omega$  impedance-matched probe head and a 0.117m coaxial sensing section with  $Z_p = 152 \Omega$ . The laboratorial measurement setup and cross-section of the coaxial sensing section are shown in Fig. 1.

Soil-under-test measured in this study are Baoshan soil (BW) and Hushan soil (LH). Baoshan soil is classified as SP-SM, which is poorly graded sand with silt with liquid limit of 29% and plastic limit of 6. Whereas Hushan soil is classified as ML, which is silt of low plasticity with liquid limit of 18% and plastic limit of 3. Both soils were remolded using target gravimetric water content (GWC) of 8%, 12% and 16% respectively. However, since the moisture control of silty soils is relatively difficult, the eventual GWC of BW soils deviated slightly from their targeted GWC, as shown in Table 1. The compacted dry density ranged from 1.765 g/cm<sup>3</sup> to 1.934 g/cm<sup>3</sup> for both soils. The measured volumetric water contents (VWC) of all soil-under-test are also computed from their corresponding GWC and dry density and are tabulated in Table 1.

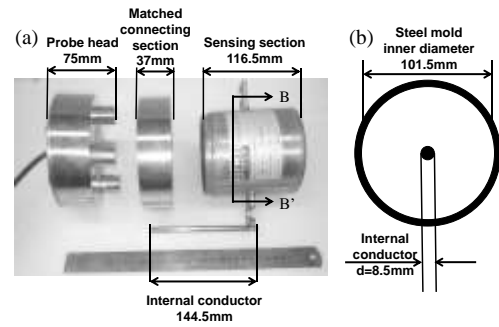


Fig. 1. (a) TDR laboratorial measurement setup. (b) Cross-section BB' of coaxial sensing section.

Table 1. State parameters of soil-under-test

Soil No.	Dry density, $\rho_{dry}$ (g/cm <sup>3</sup> )	Gravimetric water content, $\omega$ (%)	Volumetric water content, $\theta$ (%)
BW08N	1.780	10.57	18.81
BW12N	1.835	13.39	24.58
BW14N	1.765	16.01	28.25
LH08N	1.864	8.17	15.23
LH12N	1.934	12.47	24.12
LH16N	1.848	15.55	28.74

## 3 RESULTS AND DISCUSSIONS

### 3.1 Laboratorial CDP measurement of soils

Measured TDR experimental signals of all soil-under-test is shown in Fig.2. It is observed that the multiple reflections of the time domain signals for LH soils had lower reflection coefficients compared to BW soils with similar VWC. This suggested that the overall electrical conductivity (EC) of LH soils was higher than that of BW soils, which is reasonable since LH soils have higher fine contents.

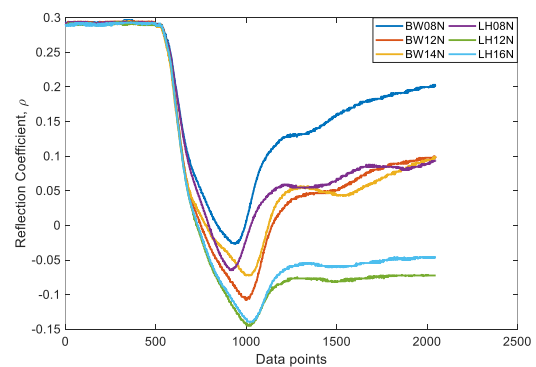


Fig. 2. Measured experimental signals of soil-under-test.

Through implementing MRA analysis on the acquired time domain signals, frequency-dependent CDP spectrums of all soil-under-test were generated through the optimization of measured MRA ratio. The selected time window for  $r_1$  started from the beginning of the truncated signal until approximately 25 data points before the lowest point of each signals. Whereas the time

window for  $r_{remaining}$  began from the same location at the end of  $r_1$  until the end of whole recorded time signal. Fast Fourier Transform (FFT) was next performed to reveal the frequency domain of both signals and their spectral ratios were compared to produce the MRA ratio. By substituting appropriate real and imaginary parts of CDP into Eq. (1) via the `fminsearch` optimization kernel of Matlab ©, the broadband CDP spectrum can hence be measured with MRA.

The inverted CDP spectrum of all soil-under-test is shown in Fig.3 and the real and imaginary parts of CDP are plotted in Fig. 3(a) and (b) respectively. Fig. 3(c) shows the zoomed in lower value range of imaginary CDP since the high EC range at low frequencies reduced the display resolution of EC at high frequencies. EC of soil-under-test mostly predominated dielectric losses and influenced the CDP spectrum up to 100 MHz. The measured MRA ratios are also shown in Fig. 4(a) for visual inspection. Workable frequency delineation line is plotted as dotted green line in Fig. 3(a), which is a function of probe sensing length and the selected time window during time domain signal extraction.

In general, soil with higher VWC value had higher values in the real part of their CDP spectrum. Dielectric constant of soil particles and air are significantly lower than water, so the amount of water in soil medium would dominate the real part of the effective CDP spectrum. Dielectric relaxation associated with bound water was observed in most soil-under-test at around 750 MHz, except for BW08N soil. Table 2 shows the coefficients of determination ( $R^2$ ) from linear regression analysis between real part of soil CDP and the corresponding VWC at each frequencies. This linear regression was performed on each soils and both soils respectively in order to investigate the difference of calibration equation in various soil types, apart from the effect of dry density. It was found that the linear correlation of CDP and VWC in both soils was the highest at 500 MHz, either regressed separately or collectively. Linear regression plots at 100 MHz and 500 MHz are shown in Fig. 4(a) and (b) respectively, demonstrating the degree of soil type dependency at both frequencies. Fig. 4(b) shows that both soils have the highest linear correlation and  $R^2$  value, indicating that the soil type dependency of  $real(\epsilon^*)$  is lowest at 500 MHz. Linear regression model established between real CDP and VWC at this frequency may therefore yield relatively accurate result.

Higher EC reduces the reflection coefficient of the steady state of time domain signals. Comparing the time domain signals of BW12N and LH12N soils that had similar VWC values, direct apparent dielectric permittivity determination from their time domain signal may result in a large VWC difference as the risetime of their second reflections were influenced by EC. However, the real part of their measured CDP spectrum via MRA approach resulted in similar values throughout their effective frequency from 150 MHz to 850 MHz. The

difference in soil mineralogy and EC affected the lower frequency region of their imaginary CDP spectrum. LH soils with relatively higher EC value resulted in larger imaginary CDP value at lower frequencies, which is the typical frequency range dominated by EC.

Generally, EC value increases as VWC increases especially for fine-grained soils. However, slight discrepancy in the EC variation of LH12N and LH16N was observed, where the inverted imaginary CDP at low frequencies of LH12N is higher than LH16N. This is the typically EC dominated frequency range and the time domain signal of both soils in Fig. 2 also reflected the same condition, where the relatively steady state section of LH12N is lower than LH16N. This inconsistency maybe due to the former soil was mixed with tap water with higher EC value. Nevertheless, MRA algorithm still managed to capture their actual electrical behavior, revealing the underlying dielectric properties of these soil-under-test.

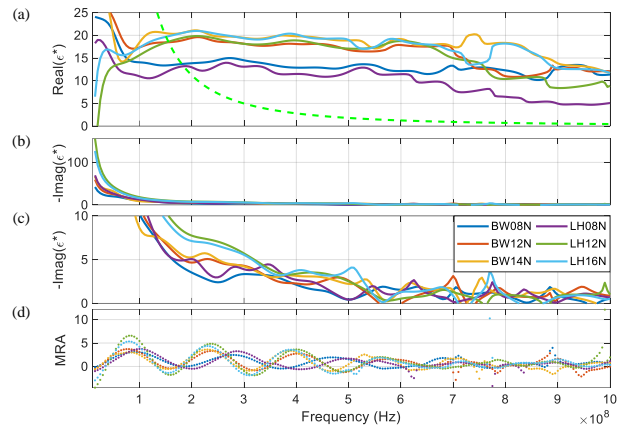


Fig. 3. Soil CDP spectrum: (a) Real part of CDP. (b) -Imaginary part of CDP. (c) -Imaginary part of CDP (zoomed in). (d) MRA ratio.

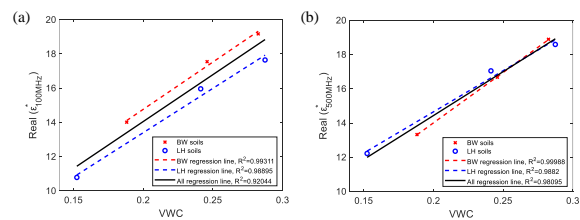


Fig. 4. Effect of soil type between the density-normalized real CDP and VWC at various frequencies: (a) 100MHz. (b) 400MHz.

Table 2. Linear regression analysis between real CDP and VWC of soil-under-test by frequency

Frequency (MHz)	$R^2$ of BW soil only	$R^2$ of LH soil only	$R^2$ of both soils
100	0.9931	0.9890	0.9204
300	0.9815	0.9750	0.9729
500	0.9999	0.9882	0.9810
700	0.9992	0.9707	0.8956
900	0.1873	0.9464	0.4505

### 3.2 Relationship between real ( $\epsilon^*$ ) to GWC

As aforementioned, the dry density of the compacted soil samples may influence the correlation between real part of CDP and GWC. This study hence normalized the real CDP spectrum by its squared value to their corresponding dry densities as shown in Fig. 5. The relative positions of the normalized CDP spectrum for each soil types became more correlated to the GWC. In order to investigate the potential of frequency range with higher density independence, similar linear regression analysis was conducted between real CDP and GWC. Similar to VWC correlation, this study found that 500 MHz was again the frequency range with the highest  $R^2$  value for the real( $\epsilon^*$ )-GWC correlation, as shown in Fig. 6(a). However, the  $R^2$  value in the GWC relationship was comparatively smaller than the VWC correlation, which is mainly attributable to the slight influence of soil density. Linear correlation analysis between the normalized CDP and GWC was next performed to study the effectiveness of density normalization to the CDP-GWC calibration function. This study discovered that the optimal frequency for the normalized CDP-GWC correlation is at 400 MHz, as shown in Fig. 6(b). This outcome is concurrent with the outcome from CDP-VWC correlation, since the ratio of VWC to GWC is directly the dry density of soil. The CDP normalization involving taking the square root of CDP also slightly increased the  $R^2$  value of the overall linear regression from 0.98095 (CDP-VWC) to 0.98414 (normalized CDP-GWC).

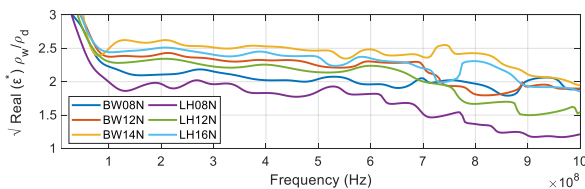


Fig. 5. Density-normalized real part of soil CDP spectrum.

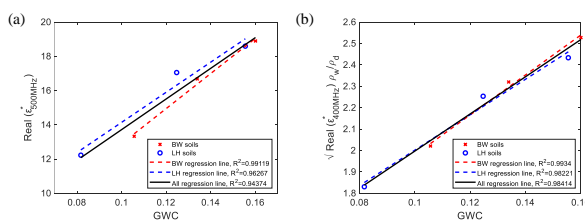


Fig. 6. Effect of soil type and dry density to the correlation between real CDP and GWC: (a) Real CDP at 500MHz. (b) Normalized real CDP at 400MHz.

### 4 CONCLUSION

This study adopted the multiple reflection analysis (MRA) approach of time domain reflectometry (TDR) signals and measured the complex dielectric permittivity (CDP) spectrum of two soil-under-test effectively. Through robust MRA algorithm, both real and imaginary parts of CDP spectrum of the compacted soil samples with various moisture content were generated from 10 MHz to 1 GHz. The frequency dependency of real part of CDP to the volumetric water content (VWC) was analyzed through linear regression. The effect of dry density to the real part of CDP was also studied by the linear correlation between the density-normalized CDP spectrum and gravimetric water content (GWC). The optimal frequency range for both linear correlations of CDP-VWC and normalized CDP-GWC was found to be 400MHz for both BW and LH soils. Effect of electrical conductivity is found in the low frequency range of imaginary CDP approximately before 100MHz. Additional soil types are recommended to be included in further study for a more comprehensive soil parameter investigation.

### ACKNOWLEDGEMENTS

This work was supported by Taiwan's Environmental Protection Administration and the Ministry of Science and Technology (under Contract No. MOST 105-2221-E-002 -063)

### REFERENCES

- Dobson, M., Ulaby, F., Hallikainen, M., and El-rayes, M. (1985). "Microwave Dielectric Behavior of Wet Soil-Part II: Dielectric Mixing Models." *IEEE Transactions on Geoscience and Remote Sensing*, GE-23(1), 35–46.
- Heimovaara, T. J. (1994). "Frequency domain analysis of time domain reflectometry waveforms: 1. Measurement of the complex dielectric permittivity of soils." *Water Resources Research*, 30(2), 189–199.
- Lin, C.-P. (2003). "Frequency domain versus travel time analyses of TDR waveforms for soil moisture measurements." *Soil Science Society of America Journal*, 67(3), 720–729.
- Lin, C.-P., Ngui, Y. J., and Lin, C.-H. (2017). "A novel TDR signal processing technique for measuring apparent dielectric spectrum." *Measurement Science and Technology*, 28(1), 015501.
- Lin, C.-P., Ngui, Y. J., and Lin, C.-H. (2018). "Multiple Reflection Analysis of TDR Signal for Complex Dielectric Spectroscopy." *IEEE Transactions on Instrumentation and Measurement*, 1–13.